

Supporting Information

Tuning of thermal quenching performance of Bi³⁺-doped scheelite
Ca(Mo/W)O₄ solid solution phosphors

Ran Xiao,^a Ning Guo,^{a,*} Xiang Lv,^a Qincan Ma,^a Baiqi Shao,^b and Ruizhuo Ouyang,^a

^a Department of Chemistry, University of Shanghai for Science and Technology, Shanghai 200093, P. R. China.

^b State Key Laboratory of Rare Earth Resource Utilization, Changchun Institute of Applied Chemistry, Chinese Academy of Sciences, Changchun 130022, P. R. China.

*Corresponding author: Tel.: +86-21-65711344; Fax: +86-21-65711344;

E-mail: guoning@usst.edu.cn

Figure S1

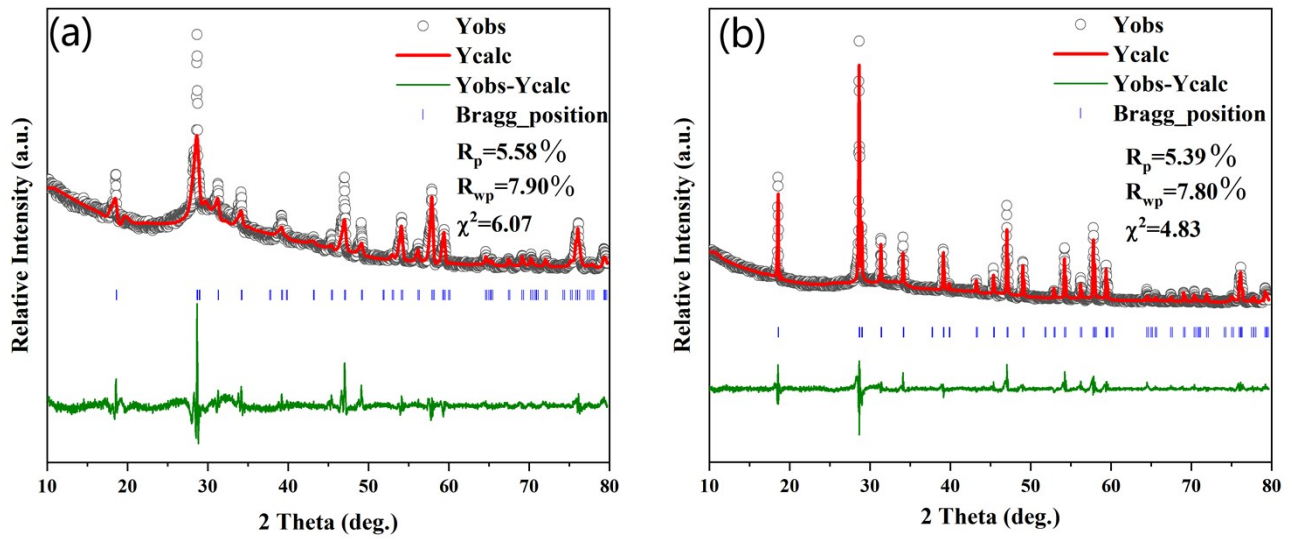


Figure S1 Rietveld refinement patterns for X-ray diffraction patterns of (a) $\text{Ca}_{0.99}\text{Mo}_{0.5}\text{W}_{0.5}\text{O}_4:0.01\text{Bi}^{3+}$
(b) $\text{Ca}_{0.99}\text{WO}_4:0.01\text{Bi}^{3+}$.

Figure S2

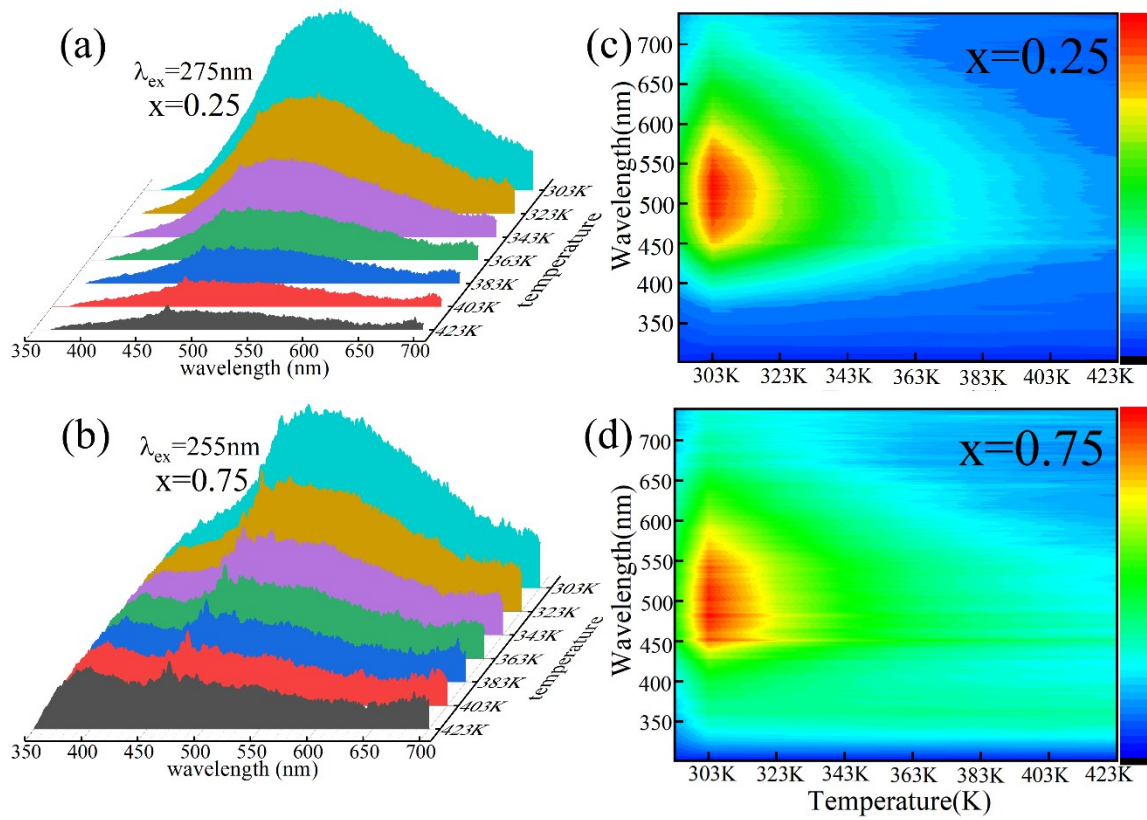


Figure S2 Emission spectra of (a, c) $\text{Ca}_{0.99}\text{Mo}_{0.75}\text{W}_{0.25}\text{O}_4:0.01\text{Bi}^{3+}$ (b, d) $\text{Ca}_{0.99}\text{Mo}_{0.25}\text{W}_{0.75}\text{O}_4:0.01\text{Bi}^{3+}$ at 303-423K.

Figure S3

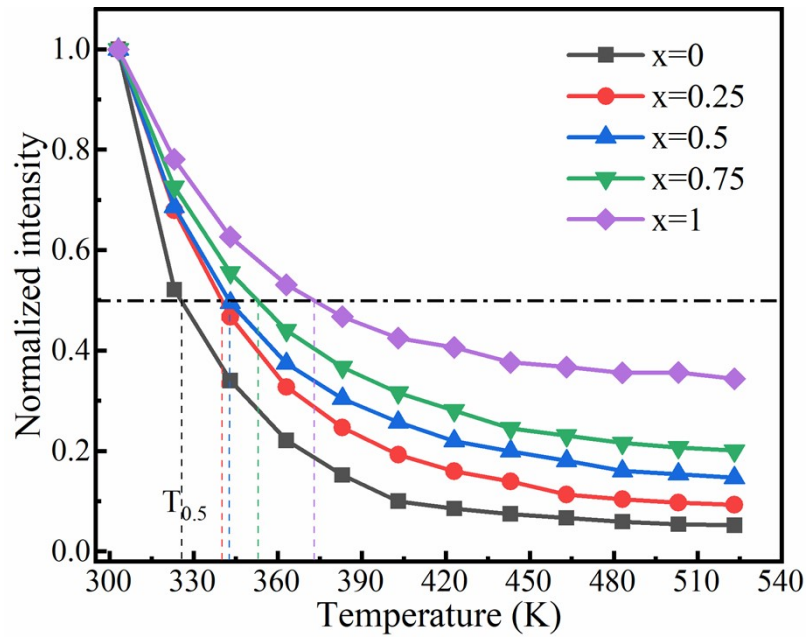


Figure S3 Normalized integrated intensity of $\text{Ca}_{0.99}\text{Mo}_{1-x}\text{W}_x\text{O}_4:0.01\text{Bi}^{3+}$ ($x=0-1$) at 303-523K

Figure S4

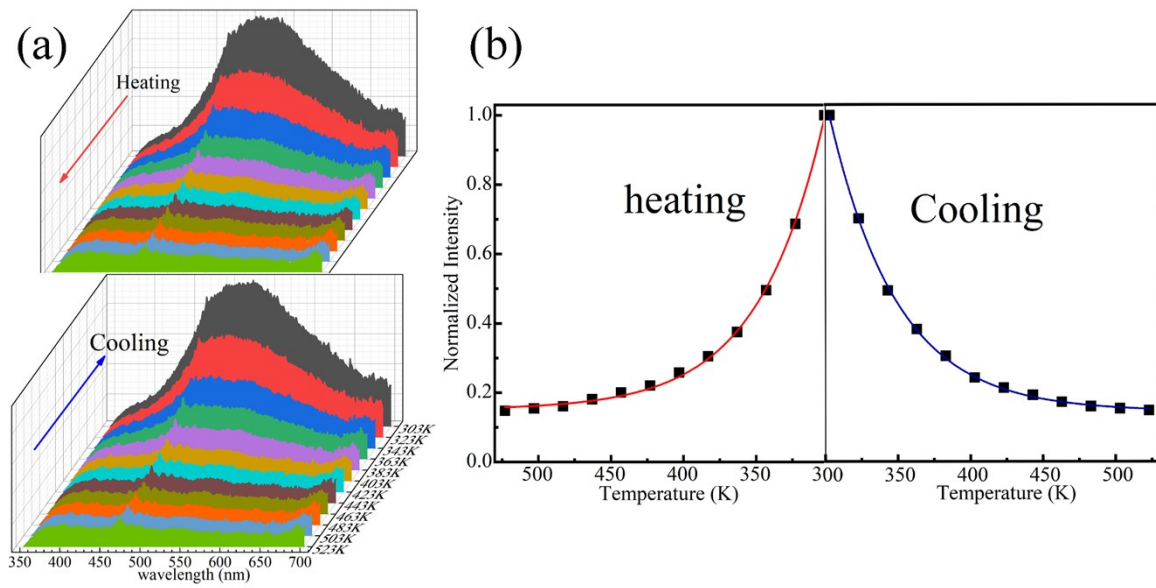


Fig. S4 (a) Emission spectra of $\text{Ca}_{0.99}\text{Mo}_{0.5}\text{W}_{0.5}\text{O}_4:0.01\text{Bi}^{3+}$ solid solution on heating and cooling at 303-523K. (b) The fitting curve of the corresponding integrated intensity.

Figure S5

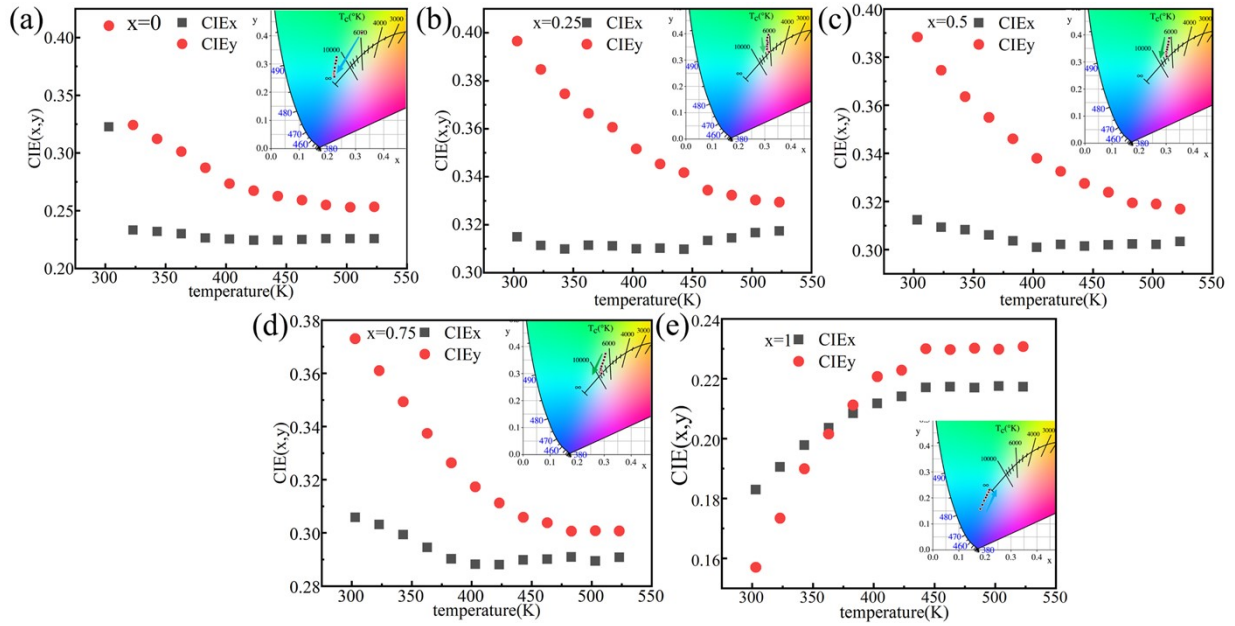


Figure S5 (a-e) $\text{Ca}_{0.99}\text{Mo}_{1-x}\text{W}_x\text{O}_4:0.01\text{Bi}^{3+}$ ($x=0, 0.25, 0.5, 0.75, 1$) in variable temperature chromaticity coordinates (x, y), and the insets are the corresponding CIE chromaticity diagrams.

Figure S6

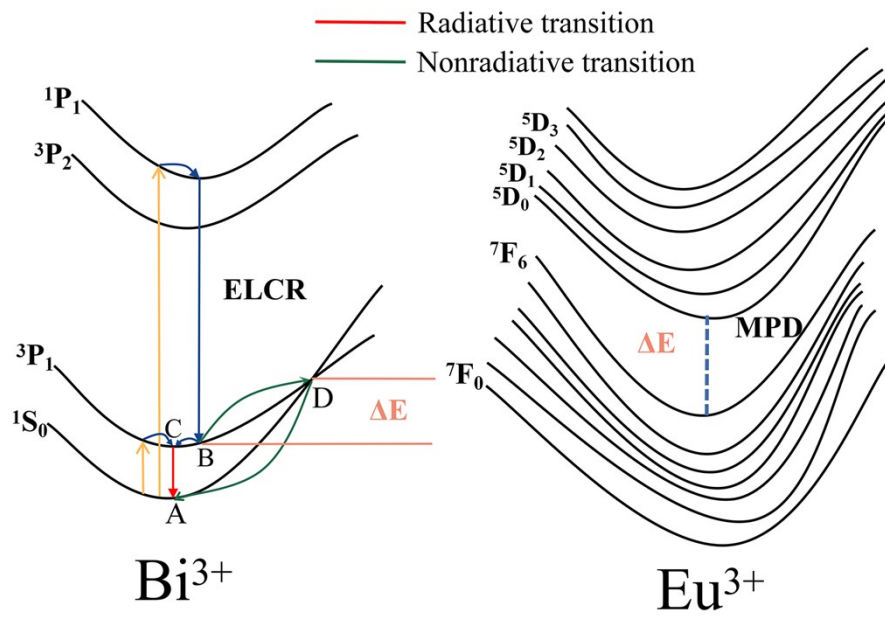


Figure S6 Schematic of the quenching mechanism for the Bi^{3+} activator and the MPD quenching for Eu^{3+} .

Figure S7

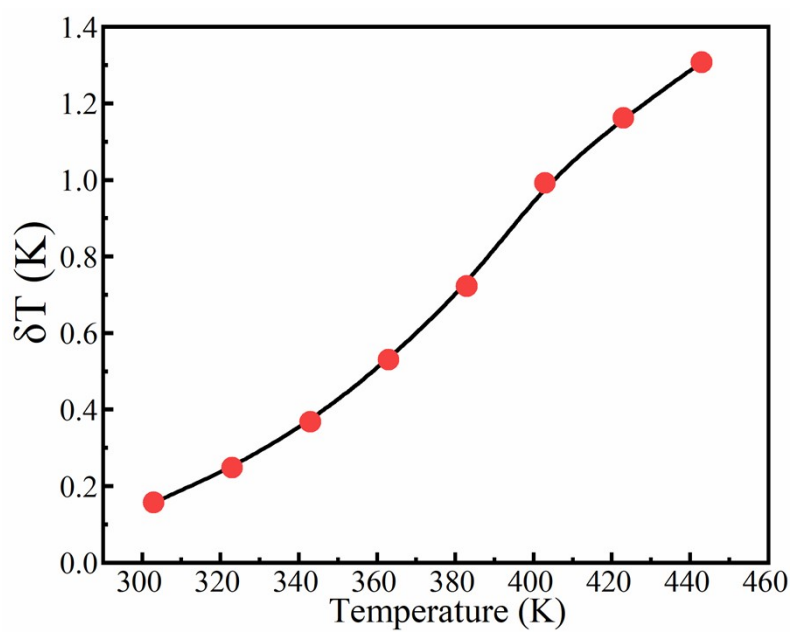


Figure S7 The temperature resolution of $\text{Ca}_{0.985}\text{Mo}_{0.5}\text{W}_{0.5}\text{O}_4:0.01\text{Bi}^{3+},0.0025\text{Eu}^{3+}$.

Table S1 The relevant Rietveld refinement parameters and crystallo-graphic data.

| Parameter | Ca _{0.99} MoO ₄ :0.01Bi ³⁺ | Ca _{0.99} Mo _{0.5} W _{0.5} O ₄ :0.01Bi ³⁺ | Ca _{0.99} WO ₄ :0.01Bi ³⁺ |
|------------------------------------|---|--|--|
| Space group | I4 ₁ /a | I4 ₁ /a | I4 ₁ /a |
| a=b (Å) | 5.22294 | 5.24020 | 5.24801 |
| c (Å) | 11.43149 | 11.42373 | 11.38946 |
| α=β=γ (deg) | 90.000 | 90.000 | 90.000 |
| Unit cell volume (Å ³) | 311.841 | 313.692 | 313.684 |
| R _p (%) | 4.99 | 5.58 | 5.39 |
| R _{wp} (%) | 6.79 | 6.70 | 7.80 |
| χ ² | 3.77 | 6.07 | 4.83 |

Table S2 Several dual rare-earth doped optical temperature measurement materials of Sa and Sr for typical temperature sensors.

| Sensing materials | Excitation wavelength(nm) | Temperature range(K) | S _r (%K ⁻¹) ¹⁾ | Sa (K ⁻¹) | Ref. |
|---|---------------------------|----------------------|--|-----------------------|-----------|
| SrY ₂ O ₄ :Bi ³⁺ ,Eu ³⁺ | 330 | 313-563 | 0.86 | 0.0433 | 1 |
| CaYZr ₂ Al ₃ O ₁₂ :Bi ³⁺ ,Eu ³⁺ | 278 | 297-573 | 0.664 | 0.00826 | 2 |
| LaScO ₃ :Bi ³⁺ ,Eu ³⁺ | 308 | 280-480 | 0.795 | 0.118 | 3 |
| NaGd(MoO ₄) ₂ :Tb ³⁺ ,Pr ³⁺ | 310 | 303-483 | 2.05 | 0.097 | 4 |
| LuNbO ₄ : Tb ³⁺ ,Pr ³⁺ | 305 | 283-493 | 1.26 | 0.024 | 5 |
| NaGdF ₄ :Yb ³⁺ ,Er ³⁺ | 980 | 303-343 | 1.29 | 0.0365 | 6 |
| GdNbO ₄ :Bi ³⁺ ,Eu ³⁺ | 308 | 303-523 | 3.81 | 0.0367 | 7 |
| Ca _{0.985} Mo _{0.5} W _{0.5} O ₄ :Bi ³⁺ ,Eu ³⁺ | 265 | 303-523 | 3.1713 | 0.06553 | This work |

Reference

1. R. Wei, J. Guo, K. Li, L. Yang, X. Tian, X. Li, F. Hu and H. Guo, Dual-emitting SrY₂O₄:Bi³⁺,Eu³⁺ phosphor for ratiometric temperature sensing, *Journal of Luminescence*, 2019, **216**, 116737.
2. Z. Zheng, J. Zhang, X. Liu, R. Wei, F. Hu and H. Guo, Luminescence and self-referenced optical temperature sensing performance in Ca₂YZr₂Al₃O₁₂:Bi³⁺,Eu³⁺ phosphors, *Ceramics International*, 2020, **46**, 6154-6159.
3. D. Huang, Y. Wei, P. Dang, X. Xiao, H. Lian and J. Lin, Tunable color emission in LaScO₃:Bi³⁺,Tb³⁺,Eu³⁺ phosphor, *Journal of the American Ceramic Society*, 2020, **103**, 3273-3285.
4. Y. Gao, F. Huang, H. Lin, J. Zhou, J. Xu and Y. Wang, A Novel Optical Thermometry Strategy Based on Diverse Thermal Response from Two Intervalence Charge Transfer States, *Advanced Functional Materials*, 2016, **26**, 3139-3145.
5. Y. Wu, H. Suo, X. Zhao, Z. Zhou and C. Guo, Self-calibrated optical thermometer LuNbO₄:Pr³⁺/Tb³⁺ based on intervalence charge transfer transitions, *Inorganic Chemistry Frontiers*, 2018, **5**, 2456-2461.
6. J. Wang, H. Lin, Y. Cheng, X. Cui, Y. Gao, Z. Ji, J. Xu and Y. Wang, A novel high-sensitive upconversion thermometry strategy: Utilizing synergistic effect of dual-wavelength lasers excitation to manipulate electron thermal distribution, *Sensors and Actuators B-Chemical*, 2019, **278**, 165-171.
7. J. Xue, H. M. Noh, B. C. Choi, S. H. Park, J. H. Kim, J. H. Jeong and P. Du, Dual-functional of non-contact thermometry and field emission displays via efficient Bi³⁺ → Eu³⁺ energy transfer in emitting-color tunable GdNbO₄ phosphors, *Chemical Engineering Journal*, 2020, **382**, 122861.